This article was downloaded by: [Manish Kumar]
On: 05 October 2013, At: 02:04
Publisher: Taylor & Francis
Informa Ltd Registered in England and Wales Registered Number: 1072954 Registered office: Mortimer House, 37-41 Mortimer Street, London W1T 3JH, UK

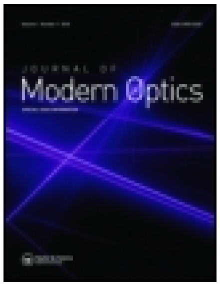

Journal of Modern Optics
Publication details, including instructions for authors and subscription information:
http://www.tandfonline.com/loi/tmop20

Comparative study of dispersion characteristics of uniaxial crystalline optical fiber under the extreme cases of helix pitch angles

A.K. Mishra[a], M. Kumar[b], D. Kumar[c] & O.N. Singh II[a]

[a] Department of Applied Physics, Indian Institute of Technology, Banaras Hindu University, Varanasi 221005, India.

[b] Department of Electrical Engineering, Indian Institute of Technology, Banaras Hindu University, Varanasi 221005, India.

[c] Faculty of Engineering, Multimedia University, Cyberjaya, Malaysia.

Published online: 03 Oct 2013.

To cite this article: A.K. Mishra, M. Kumar, D. Kumar & O.N. Singh II , Journal of Modern Optics (2013): Comparative study of dispersion characteristics of uniaxial crystalline optical fiber under the extreme cases of helix pitch angles, Journal of Modern Optics, DOI: 10.1080/09500340.2013.833316

To link to this article: http://dx.doi.org/10.1080/09500340.2013.833316

PLEASE SCROLL DOWN FOR ARTICLE

Taylor & Francis makes every effort to ensure the accuracy of all the information (the “Content”) contained in the publications on our platform. However, Taylor & Francis, our agents, and our licensors make no representations or warranties whatsoever as to the accuracy, completeness, or suitability for any purpose of the Content. Any opinions and views expressed in this publication are the opinions and views of the authors, and are not the views of or endorsed by Taylor & Francis. The accuracy of the Content should not be relied upon and should be independently verified with primary sources of information. Taylor and Francis shall not be liable for any losses, actions, claims, proceedings, demands, costs, expenses, damages, and other liabilities whatsoever or howsoever caused arising directly or indirectly in connection with, in relation to or arising out of the use of the Content.

This article may be used for research, teaching, and private study purposes. Any substantial or systematic reproduction, redistribution, reselling, loan, sub-licensing, systematic supply, or distribution in any form to anyone is expressly forbidden. Terms & Conditions of access and use can be found at http://www.tandfonline.com/page/terms-and-conditions

Journal of Modern Optics, 2013
http://dx.doi.org/10.1080/09500340.2013.833316

Comparative study of dispersion characteristics of uniaxial crystalline optical fiber under the extreme cases of helix pitch angles

A.K. Mishra[a]*, M. Kumar[b], D. Kumar[c] and O.N. Singh II[a]

[a]*Department of Applied Physics, Indian Institute of Technology, Banaras Hindu University, Varanasi 221005, India;* [b]*Department of Electrical Engineering, Indian Institute of Technology, Banaras Hindu University, Varanasi 221005, India;* [c]*Faculty of Engineering, Multimedia University, Cyberjaya, Malaysia*

(*Received 22 May 2013; accepted 5 August 2013*)

Some special cases of dispersion characteristics of a uniaxial crystalline optical fiber with a helical winding on the core-cladding boundary are investigated theoretically. In the present case, the optical fiber is doubly unconventional: (i) in the choice of uniaxial crystalline optical fiber and (ii) in the choice of sheath helix between the core and cladding. Field components, boundary conditions, and eigenvalue equations for HE and EH modes are obtained. We consider two special cases, i.e. $\psi = 0°$ and $\psi = 90°$ to obtain simpler eigenvalue equations which contain Bessel and modified Bessel functions and their derivatives. The nature of the dispersion curve remains unaffected with the anisotropy and only cutoff frequency is lowered for the positive uniaxial crystals. The helix pitch angle does not affect the modal cutoffs but it effectively controls the number of guided modes. This property has promising importance in long-distance communication where only a few modes are desired to be guided in order to minimize the inter-modal dispersion.

Keywords: hybrid mode; anisotropic parameter; modal dispersion; pitch angle

Downloaded by [Manish Kumar] at 02:04 05 October 2013

1. Introduction

Important anisotropic media are generally crystalline and their properties are closely related to various symmetry properties possessed by crystals. Anisotropic crystals have fascinated engineers and scientists as the key materials of optoelectronics, integrated optics, and other technical fields of application due to their marked properties of rigidity, directionality, and mechanical strength [1]. With the passage of crystal development techniques, optical fibers with a crystalline anisotropic core were proposed and investigated to take advantage of their directional oriented properties in fiber couplers and fiber Bragg waveguides [2–4]. Wave propagation along a cylindrically symmetric step-index fiber with the core and cladding made of uniaxial crystal was studied by Toning [5] and a simpler and more exact analysis was carried out on the basis of modal theory [6–8] when the fiber is under the weak guidance approximation. The surface impedance/admittance approach, which is valuable to study the reflection of waves at plane interfaces, was adopted to investigate the condition of wave propagation in a planar waveguide for the uncoupled TE and TM modes [9]. A transmission line approach was also considered by some workers [10] to explain the guidance of nonlinear waves through slab waveguides with a complex refractive index. The coupling of guided modes with the unguided radiation modes leads to leaky modes which ultimately exhibits loss and such type of couplings are not desirable. The effect of anisotropy on leaky mode loss and modal coupling for planar and non-planar structures were studied by several workers [11,12] employing the coupled mode and beam propagation theory.

The helical slow wave structures fall under unconventional complex waveguide structures, accompanying the many distinct characteristics over the conventional cylindrical waveguides and periodic structures, and are widely used in the field of travelling wave tubes (TWTs) [13–15]. The slowing down characteristics of a helix make it suitable for broad band amplification and the coupling of slow modes with an electron beam, which generates coherent short wavelength radiation. In helical structures, the wave propagating perpendicular to helical windings (i.e. along the waveguide axis) propagates as if it had been confined in a periodic bounded medium, but the EM radiation propagating along the helical turns does not encounter any periodic boundaries. Thus, the helices have unique characteristics of aperiodicity along the helical turns as compared to other periodic structures. According to Floquet's theorem, the periodicity of a structure can not be defined only on the basis of

*Corresponding author. Email: onkar_akm@yahoo.co.in

© 2013 Taylor & Francis

Downloaded by [Manish Kumar] at 02:04 05 October 2013

translational symmetry; instead, other symmetry considerations must also be taken into account [15]. For instance, if one moves a small distance along the helical wire and then rotate an appropriate angle, the helix becomes congruent to itself, which clearly justifies the absence of periodicity in the helical direction. Keeping in view the widespread application of helices in TWTs, an almost new kind of optical fiber with helical windings was proposed and analyzed by Singh et al. [16] and the effect of tapering on field variations was also investigated for such types of waveguides [17]. Their studies showed that such types of optical fibers display unusual dispersion characteristics that are strongly dependent on the helix pitch angle.

Considering the aforesaid investigations, we have proposed the helically cladded cylindrical dielectric waveguide with crystalline anisotropic core. Alternatively, one may consider it to be a dielectric-loaded wave tube in which the central guiding region is crystalline. The purpose of the present communication is to explore the effect of helical winding and anisotropy of the media on the propagation characteristics of optical fiber based on the modal theory. The dispersion relation for hybrid modes (HE and EH) are separately deduced and the effect of anisotropy on the modal dispersion is extensively investigated. The anisotropy character of the media is introduced through a permittivity tensor subject to the existence of cylindrical symmetry. The motivation behind such a complex waveguide structure stems from the considerations of the characteristics of electrons propagating through a tube over which there is a helical winding. The presence of a helical boundary at the core–cladding interface modifies the dispersion relation and, hence, may affect the modal behavior.

This paper is analytical in nature and its approach concerns mainly a theoretical study. Although the pitch angle ψ (angle made by helical turns with normal to the waveguide axis) can take any arbitrary value between 0° and 90°, we are only interested here to consider the extreme cases of pitch angles (0° and 90°). These pitch angles are purposely considered as they represent the two extreme states of helices. For the first pitch angle, the helix assumes the shape of a ring, while for the latter case it transforms into the shape of an open helix in which the helical wires are parallel to the waveguide axis**.** The helical windings are right-handed here, and the direction of propagation is the positive z-direction. The case of a sheath helix, which can be realized by many similar windings tightly bound side by side but insulated from each other, is considered. Equivalently, one can consider it as a cylindrical surface, which has the property of conduction only in the helical direction but not in the perpendicular direction. Our present communication concerns only on the discussion of hybrid modes since in helically cladded step-index optical fibers, the cylindrically symmetric TE and TM modes do not exist [16]. There is vast literature [18,19] on the classification scheme of modes, but in our present manuscript we will follow the procedure of classification of modes suggested by Snitzer [20].

2. Mathematical formulations

To develop the mathematical background of the proposed structure, we consider the periodic variation of fields in time, phase and frequency as $e^{j(\omega t-\beta z+v\theta)}$, where ω is the angular frequency, β is the longitudinal propagation constant and θ is the phase constant. We consider a helically cladded crystalline anisotropic (uniaxial) optical fiber in which the z-axis is the direction of wave propagation and the profile of refractive index is step like. The physical layout of the structure under investigation is shown in Figure 1. The electromagnetic properties of the media are characterized by its permittivity and permeability and are sufficiently accurately defined by

$$\bar{\varepsilon} = \begin{bmatrix} \varepsilon_{xx} & 0 & 0 \\ 0 & \varepsilon_{yy} & \varepsilon_{yz} \\ 0 & \varepsilon_{zy} & \varepsilon_{zz} \end{bmatrix}, \tag{1}$$

where a bar over the function ε represents its tensor nature and the permeability (μ) of the media assumes its free space value since the crystal is assumed to be non-gyrotropic. An analytical solution of the wave equation is possible only when the waveguide axis (z-axis) and the optic axis of the crystal are collinear [2], so we will retain these assumptions in our analysis. Due to cylindrical symmetry, the off-diagonal elements of the permittivity matrix are equal and these are assumed to be zero since these off-diagonal elements couple the guided modes with unguided radiation modes, which ultimately leads to coupling losses [7,12]. Thus, the reduction of the permittivity tensor to a diagonal dielectric matrix is the better possible structure for the analytical study of guided modes. Furthermore, we assume that the principal axis of the dielectric tensor is aligned with the waveguide axis and that dielectric constants are spatially

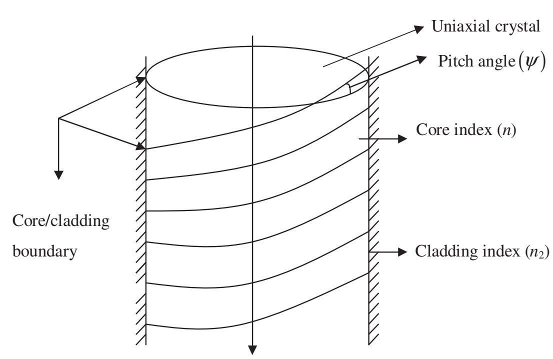

Figure 1. Geometry of helically cladded fiber with crystalline anisotropic core.

isotropic. In the case of isotropic media, the **D** and **E** vectors are parallel to each other and, hence, the divergence of **D** is zero. However, for anisotropic media, we have from Maxwell's equation

$$\nabla \cdot D = (\nabla \bar{\bar{\varepsilon}}) \cdot E + \bar{\bar{\varepsilon}} (\nabla \cdot E) = 0. \tag{2}$$

But for homogeneous media, **div E** is zero. Simplification of the above equation leads to

$$\nabla \cdot E = \left(1 - \frac{\varepsilon_z}{\varepsilon_t}\right) \frac{\partial E_z}{\partial z} \neq 0, \tag{3}$$

which clearly means that the **D** and **E** vectors are antiparallel. The derivations of wave equation in the core and cladding regions of optical fiber involves the routine procedure of using basic Maxwell's equations along with the method of separation of variables with some algebraic manipulations.

Assuming n_t and n_z to be the refractive indices of the crystal in transverse and longitudinal directions, respectively, and that n_2 is the refractive index of the cladding, the propagation constant of any mode for this structure is restricted within the limit $k\, n_t \geq \beta \geq k\, n_2$. Defining the propagation parameters as

$$k_t = \sqrt{k^2 n_t^2 - \beta^2}, \tag{4}$$

$$k_z = \frac{n_z}{n_t} k_t = \delta\, k_t, \tag{5}$$

$$w = \sqrt{\beta^2 - k^2 n_2^2}, \tag{6}$$

all the field components can be expressed in terms of familiar Bessel's functions and these are listed in Table 1. A Bessel function of the first kind (J_ν) has been used in the core region to represent the oscillating nature of fields, while a modified Bessel function of the second kind (K_ν) is used to preserve the decaying character. From Equations (4) and (6), the following parameters can be identified:

$$a^2\, k_t^2 + a^2\, w^2 = \delta^2 a^2\, k_z^2 + a^2\, w^2 = V^2, \tag{7}$$

$$b = \frac{a^2\, w^2}{a^2\, k_t^2 + a^2\, w^2} = \frac{W^2}{V^2}, \tag{8}$$

where V is the normalized frequency and b is the normalized propagation constant. Recasting the definitions of numerical aperture (NA) and V number, these can be expressed as

$$NA = \sqrt{n_t^2 - n_2^2} = n_t \sqrt{1 - \frac{\delta^2 n_2^2}{n_z^2}} = n_t \sqrt{1 - \xi^2}, \tag{9}$$

$$V = k\, a\, NA. \tag{10}$$

From Equations (9 and 10), it is evident that for a fixed value of n_t, a change in δ leads to the corresponding change in n_z according to Equation (5) and hence ξ remains constant. Thus, the NA and hence V number remain essentially constant whatever the value of n_z may be. Thus, those anisotropic crystals which have higher value of n_t will have higher light gathering capacity.

In our present study, we consider a sheath helix model in which very fine wires of infinite conductivity are separated from each other by a dielectric material. This assumption is valid only for very fine wires of infinitely small transverse dimension [16]. One may use a tape helix model by taking into account the finite width of wire. In this case, fields are expanded with the help of Floquet's theorem [14]. Applying the sheath helix boundary conditions (Table 2) at the core–cladding interface in

Table 1. Field components in core and cladding regions of optical fiber.

Core region ($r \leq a$)	Cladding region ($r > a$)
$E_{z_1} = A\, J_\nu(k_z r)\, e^{j\nu\theta}$	$E_{z_2} = C\, K_\nu(w\, r)\, e^{j\nu\theta}$
$H_{z_1} = B\, J_\nu(k_t r)\, e^{j\nu\theta}$	$H_{z_2} = D\, K_\nu(w\, r)\, e^{j\nu\theta}$
$E_{r_1} = -\frac{j\beta}{k_t^2}\left\{A\, k_z\, J'_\nu(k_z\, r) + B\frac{j\omega\,\mu\,\nu}{\beta\, r} J_\nu(k_t\, r)\right\} e^{j\nu\theta}$	$E_{r_2} = \frac{j\beta}{w^2}\left\{C\, w\, K'_\nu(w\, r) + D\frac{j\omega\,\mu\,\nu}{\beta\, r} K_\nu(w\, r)\right\} e^{j\nu\theta}$
$H_{r_1} = -\frac{j\beta}{k_t^2}\left\{B\, k_t\, J'_\nu(k_t\, r) - A\frac{j\omega\,\nu\, n_1^2}{\beta\, r} J_\nu(k_z\, r)\right\} e^{j\nu\theta}$	$H_{r_2} = \frac{j\beta}{w^2}\left\{D\, w\, K'_\nu(w\, r) - C\frac{j\omega\,\nu\, n_2^2}{\beta\, r} K_\nu(w\, r)\right\} e^{j\nu\theta}$
$E_{\theta_1} = -\frac{j\beta}{k_t^2}\left\{A\frac{j\nu}{r} J_\nu(k_z\, r) - B\frac{\omega\mu\, k_t}{\beta} J'_\nu(k_t\, r)\right\} e^{j\nu\theta}$	$E_{\theta_2} = \frac{j\beta}{w^2}\left\{C\frac{j\nu}{r} K_\nu(w\, r) - D\frac{\omega\mu\, w}{\beta} K'_\nu(w\, r)\right\} e^{j\nu\theta}$
$H_{\theta_1} = -\frac{j\beta}{k_t^2}\left\{B\frac{j\nu}{r} J_\nu(k_t\, r) + A\frac{k_z\omega\,\varepsilon_t}{\beta} J'_\nu(k_z\, r)\right\} e^{j\nu\theta}$	$H_{\theta_2} = \frac{j\beta}{w^2}\left\{D\frac{j\nu}{r} K_\nu(w\, r) + C\frac{\omega\, w\, n_2^2}{\beta} K'_\nu(w\, r)\right\} e^{j\nu\theta}$

Downloaded by [Manish Kumar] at 02:04 05 October 2013

Table 2. Helix boundary conditions [16].

$E_{Z_1}\,sin\,\psi + E_{\theta_1}\,cos\,\psi = 0$
$E_{Z_2}\,sin\,\psi + E_{\theta_2}\,cos\,\psi = 0$
$E_{Z_1}\,cos\,\psi - E_{\theta_1}\,sin\,\psi - E_{Z_2} cos\,\psi + E_{\theta_2}\,sin\,\psi = 0$
$H_{Z_1}\,sin\,\psi - H_{\theta_1}\,cos\,\psi - H_{Z_2} sin\,\psi - H_{\theta_2}\,cos\,\psi = 0$

the usual way, the eigenvalue equation for helically cladded crystal cored optical fiber comes out to be

$$\begin{aligned}
&\frac{2\,\beta\,\nu}{w^2\,k_t\,a} J_\nu(k_z a)\,J_\nu'(k_t a)\,K_\nu^2(w\,a)\ \sin\,\psi\ \cos\,\psi \\
&-\frac{J_\nu(k_z a)\,J_\nu'(k_t a)\,K_\nu^2(w\,a)}{k_t}\sin^2\psi \\
&-\frac{\beta^2\,\nu^2}{w^4\,k_t\,a^2} J_\nu(k_z a)\,J_\nu'(k_t a)\,K_\nu^2(w\,a)\ \cos^2\,\psi \\
&-\frac{J_\nu(k_z a)\,J_\nu(k_t a)\,K_\nu(w\,a) K_\nu'(w\,a)}{w}\sin^2\psi \\
&-\frac{2\,\beta\,\nu}{k_t^2\,w\,a} J_\nu(k_z a)\,J_\nu(k_t a)\,K_\nu(w\,a)\,K_\nu'(w\,a)\ \sin\,\psi\ \cos\,\psi \\
&-\frac{\beta^2\,\nu^2}{k_t^4\,w\,a^2} J_\nu(k_z a)\,J_\nu(k_t a)\,K_\nu(w\,a)\ K_\nu'(w\,a)\ \cos^2\,\psi \\
&+\frac{k^2\,n_2^2}{w^2\,k_t} J_\nu(k_z a)\,J_\nu'(k_t a)\,K_\nu'^2(w\,a)\ \cos^2\,\psi \\
&+\frac{k^2\,n_t n_z}{k_t^2\,w} J_\nu'(k_z a)\,J_\nu'(k_t a)\,K_\nu(w\,a)\,K_\nu'(w\,a)\cos^2\,\psi\ =\ 0.
\end{aligned} \tag{11}$$

This is the standard characteristic equation which is valid for all type of modes supported by the waveguide. The discussion of particular types of waveguide modes is rather restrictive and their discussion requires separate analyses.

The analysis of hybrid waveguide modes is of particular interest since the cylindrically symmetric modes are not supported by the helically cladded step-index optical fibers [16]. Using the Bessel function identities

$$\frac{J_\nu'(u\,a)}{u\,J_\nu(u\,a)} = \pm\frac{J_{\nu\mp 1}(u\,a)}{u\,a\,J_\nu(u\,a)} \mp \frac{\nu}{a\,u^2}, \tag{12}$$

$$\frac{K_\nu'(w\,a)}{w\,K_\nu(w\,a)} = \frac{K_{\nu\pm 1}(w\,a)}{w\,a\,K_\nu(w\,a)} \mp \frac{\nu}{a\,w^2}. \tag{13}$$

The dispersion relation for HE modes of the waveguide under consideration reduces to

$$\begin{aligned}
&P\,J_\nu(k_z a)\,K_\nu^2(w\,a)\left\{\frac{J_{\nu-1}(k_t a)}{k_t a} - \frac{\nu}{a\,k_t^2} J_\nu(k_t a)\right\} \\
&+R\,J_\nu(k_z a)\,J_\nu(k_t a)\,K_\nu(w\,a)\left\{\frac{K_{\nu+1}(w\,a)}{w\,a} - \frac{\nu}{a\,w^2} K_\nu(w\,a)\right\} \\
&+\left(\frac{J_{\nu-1}(k_t a)}{k_t a} - \frac{\nu}{a\,k_t^2} J_\nu(k_t a)\right)\left(\frac{K_{\nu+1}(w\,a)}{w\,a} - \frac{\nu}{a\,w^2} K_\nu(w\,a)\right) \\
&\times\cos^2\psi\left\{k^2 n_2^2\,J_\nu(k_z a)\left(\frac{K_{\nu+1}(w\,a)}{w\,a} - \frac{\nu}{a\,w^2} K_\nu(w\,a)\right)\right. \\
&\left.+\frac{k^2 n_t n_z}{k_t} K_\nu(w\,a)\left(\frac{J_{\nu-1}(k_z a)}{a} - \frac{\nu}{a\,k_z} J_\nu(k_z a)\right)\right\} = 0,
\end{aligned} \tag{14}$$

where

$$P = \left(-\sin^2\psi + \frac{2\beta\nu}{a\,w^2}\sin\psi\,\cos\psi - \frac{\beta^2\,\nu^2}{a^2\,w^4}\cos^2\psi\right)$$

and

$$R = -\left(\sin^2\psi + \frac{2\beta\nu}{a\,k_t^2}\sin\psi\,\cos\psi + \frac{\beta^2\,\nu^2}{a^2\,k_t^4}\cos^2\psi\right).$$

Similarly, the dispersion relation for EH modes follows

$$\begin{aligned}
&P\,J_\nu(k_z a)\,K_\nu^2(w\,a)\left\{-\frac{J_{\nu+1}(k_t a)}{k_t a} + \frac{\nu}{a\,k_t^2} J_\nu(k_t a)\right\} \\
&+R\,J_\nu(k_z a)\,J_\nu(k_t a)\,K_\nu(w\,a)\left\{\frac{K_{\nu-1}(w\,a)}{w\,a} + \frac{\nu}{a\,w^2} K_\nu(w\,a)\right\} \\
&+\left(-\frac{J_{\nu+1}(k_t a)}{k_t a} + \frac{\nu}{a\,k_t^2} J_\nu(k_t a)\right)\left(\frac{K_{\nu-1}(w\,a)}{w\,a} + \frac{\nu}{a\,w^2} K_\nu(w\,a)\right) \\
&\times\cos^2\psi\left\{k^2 n_2^2\,J_\nu(k_z a)\left(\frac{K_{\nu-1}(w\,a)}{w\,a} + \frac{\nu}{a\,w^2} K_\nu(w\,a)\right)\right. \\
&\left.+\frac{k^2 n_t n_z}{k_z} K_\nu(w\,a)\left(-\frac{J_{\nu+1}(k_z a)}{a} + \frac{\nu}{a\,k_z} J_\nu(k_z a)\right)\right\} = 0.
\end{aligned} \tag{15}$$

3. Numerical analysis

To analyze the dispersion characteristics of helically clad crystalline optical fiber, we take the following parameters for the judicial description of dispersion of hybrid modes: core radius (a) = 5 µm; operating wavelength (λ) = 1.55 µm; transverse component of refractive index (n_t) = 2.2866; longitudinal component of refractive index $n_z = \delta\, n_t$.

In Figures 2–7, the dispersion curves are plotted between normalized propagation constant (b) and normalized frequency (V) for some lowest order hybrid modes for different values of δ and different helix pitch angles (ψ). The pitch angle ψ = 90° corresponds to the case of an open helix in which helical wires are parallel

Downloaded by [Manish Kumar] at 02:04 05 October 2013

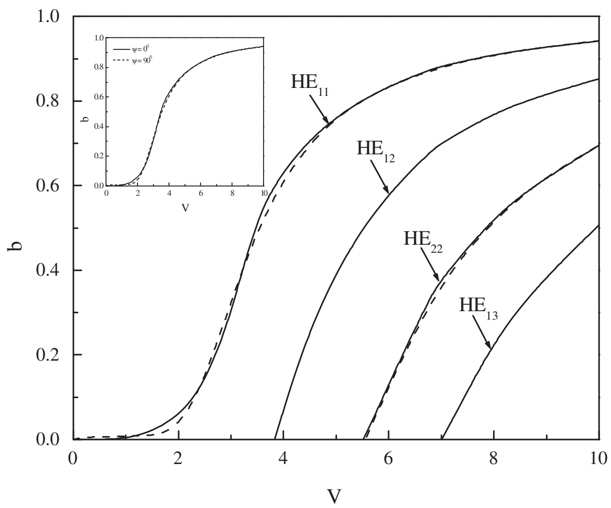

Figure 2. Dispersion curve of HE modes for anisotropic parameter ($\delta \sim 1$). Solid lines are for $\psi = 0°$ and broken lines are for $\psi = 90°$.

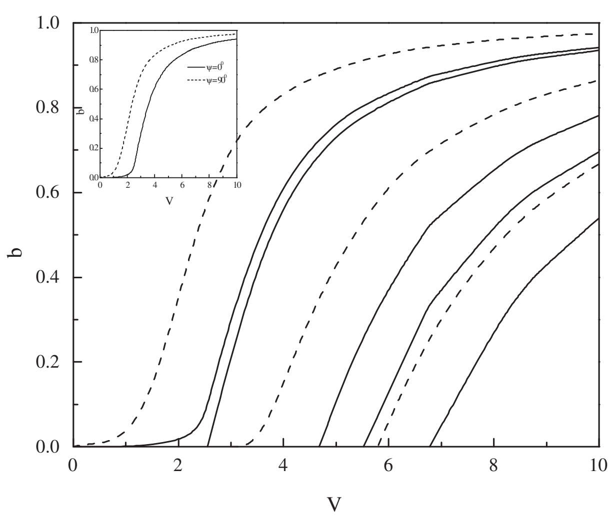

Figure 3. Dispersion curve of HE modes for anisotropic parameter ($\delta = 1.5$). Solid lines are for $\psi = 0°$ and broken lines are for $\psi = 90°$.

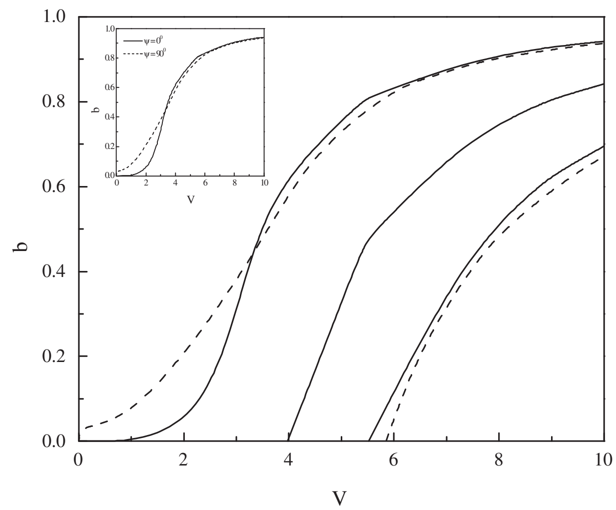

Figure 4. Dispersion curve of HE modes of negative uniaxial crystal ($LiNbO_3$) having $n_z = 2.2028$, $n_t = 2.2866$. Solid lines are for $\psi = 0°$ and broken lines are for $\psi = 90°$.

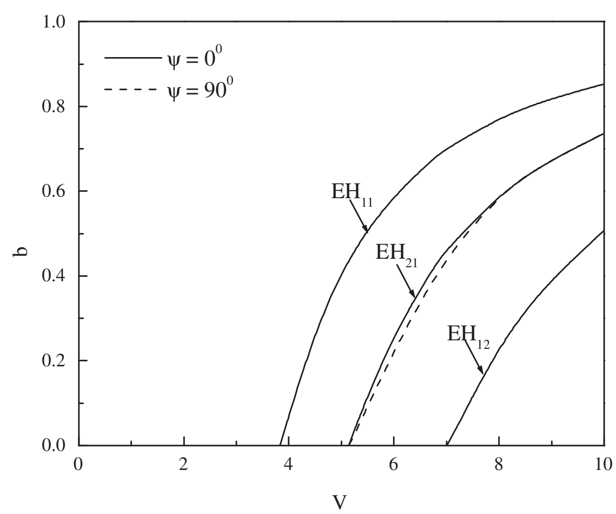

Figure 5. Dispersion curve of EH modes for anisotropic parameter ($\delta \sim 1.0$).

to the waveguide axis (z-axis). The propagation characteristics of guided modes depend exclusively on the excitation frequency, dimension of the waveguide and the refractive index of the media. In anisotropic media, the refractive index (RI) is not a constant instead it has different values in different directions, which eventually leads to the different phase velocities in different directions. The light wave advancing along the crystal axis with high value of RI is termed as an ordinary wave or o-wave and those travelling along the lower RI axis are called extraordinary or e-waves. The crystal axes corresponding to o-wave and e-wave are, respectively, the slow and fast axes. The splitting of light into ordinary and extraordinary rays leads to the modal birefringence phenomenon. Furthermore, when the optic axis and one of crystal axes are co-aligned and the wave propagates along the optic axis, the phenomenon of birefringence does not persist [8]. In our case, the z-axis is taken as the direction of wave propagation and optic axis of the crystal is also aligned along this axis. It is evident from the dispersion curves that the number of modes supported by the waveguide is strongly dependent on the anisotropic parameter (δ). Increasing δ leads to an increase in the number of modes supported and vice versa. When δ is increased from 1 (the case of +ve uniaxial media), the cutoff frequency of modes shifts to

Downloaded by [Manish Kumar] at 02:04 05 October 2013

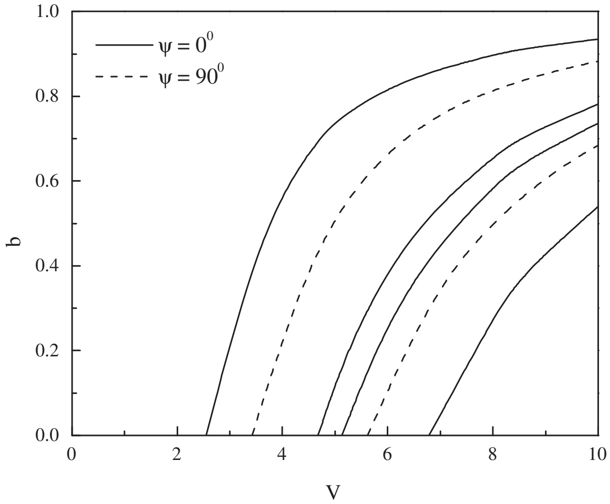

Figure 6. Dispersion curve of EH modes for anisotropic parameter (δ = 1.5).

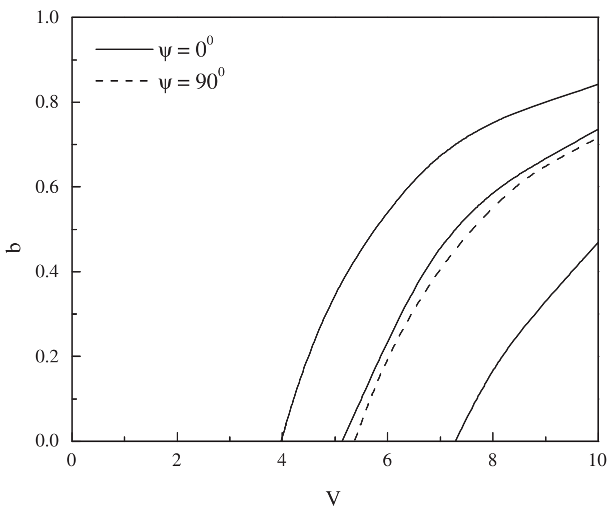

Figure 7. Dispersion curve of EH modes of negative uniaxial crystal with the parameters taken in Figure 4.

lower V-value, keeping the nature of dispersion curves intact. The cutoff frequency of guided modes is defined below

$$f_c = \frac{\kappa_{vm}}{2\,\pi\,a\,\sqrt{\mu_0(n_t - n_2)}}, \tag{16}$$

where v and m are the respective angular and radial mode orders. For a fixed value of n_t, an increase in δ causes an increase in n_z and, hence, the cutoff frequency of modes lowers. The modal dispersion profile of the fundamental mode HE_{11} is shown in the inset of Figures 2–4 for different δ values. Moreover, when δ = 1 (the case of isotropic media), the dispersion nature of the fundamental mode is nearly a replica of itself for the pitch angles ψ = 0° and ψ = 90° but when δ is different from unity, these are well separated from each other. In the dispersion curve (Figure 3), the two closely spaced solid lines displays the dispersion of two different modes for the pitch angle 0°. The first one is for the fundamental mode and second one is for the next higher mode. The discussions of cylindrically symmetric modes (TE_{0m} and TM_{0m}) are intentionally left since these modes do not exist in helically clad step-index optical fiber [16].

In Figures 5–7, the dispersion curves for hybrid EH modes are shown. In this case, the nature of the dispersion curves is also usual as for the isotropic optical fiber but the mode cutoffs and the number of modes supported are strongly dependent on δ. In Figures 4 and 7, the dispersion curves are shown, respectively, for HE and EH modes for negative uniaxial crystal ($LiNbO_3$) which has the longitudinal component of refractive indices smaller than the transverse component and is one of the most valuable crystals in integrated optical technology**.** In such kind of fibers, the modal cutoff frequency shifts to higher V value and, hence, such kind of optical waveguides can be operated as a single mode guide at higher frequencies. Moreover, it is also interesting to note from these dispersion curves that the number of modes supported is unequal for the winding pitch angles ψ = 0° and ψ = 90°. The number of modes supported is higher in the first case and the mode cutoffs are unaffected by ψ, which is in agreement with the work of Singh et al. [16]. Their effects on the dispersion characteristics are more pronounced since the dispersion relation is largely modified in these cases of pitch angles. The other pitch angles have only very insignificant impact on the modal dispersion because the normalized propagation constant is only slightly enhanced on increasing the pitch angle. Further, it is fairly evident that when the anisotropy is weak ($\delta \approx 1$), the modes are usually explainable, somewhat similar to isotropic optical fibers, but when it is strong their designations are quite difficult. Also, under the weak anisotropy condition, the polarization effects are unimportant but when the anisotropy is strong, polarization effects play a vital role [1].

4. Conclusions

The light gathering capacity of a fiber can be improved by selecting anisotropic crystals which have higher values of the transverse component of refractive index. The dispersion curves of hybrid modes display the normal expected behavior and the cutoff frequency only shifts towards lower V values on increasing n_z. This change in cutoff frequency of modes occurs for both positive and negative uniaxial crystals. The helical windings do not affect the modal cutoffs but the number of guided modes is adversely affected by ψ. Apart from this, the pitch

Downloaded by [Manish Kumar] at 02:04 05 October 2013

angle enables us to have an additional parameter to control the dispersion behavior of modes. The transition from single mode fiber to multimode fiber occurs at lower V for the +ve uniaxial crystal but these transition shifts at relatively high V for –ve crystal. This character has potential applications in the field of communication where the size of core plays a crucial role in the interfacing with other associated devices. Although, such a type of optical fiber is not physically available, we expect that with the advancement in technological improvements these analyses would yield significant, verifiable and useful information.

References

[1] Yariv, A.; Pochhi, Y. *Optical Waves in Crystals: Propagation and Control of Laser Radiation*; John Wiley & Sons: New York, 2002.

[2] Cozens, J.R. *Electron. Lett.* **1976,** *12,* 413–416.

[3] Xiaoping, Z.; Zhihong, T. *Opt. Commun*. **2002,** *204,* 127–136.

[4] Hou, S.I.; Qi, X.Q. *Chin. J. Quantum Electron.* **2005,** *22,* 642–645.

[5] Toning, A. *IEEE Trans. Microwave Theory Tech.* **1982,** *30,* 790–794.

[6] Ciattoni, A.; Cincotti, G.; Palma, C. *J. Opt. Soc. Am.* **2002,** *19,* 792–796.

[7] Lu, M.; Fejer, M.M. *J. Opt. Soc. Am.* **1993,** *10,* 246–261.

[8] Dai, J.D.; Jen, C.K. *J. Opt. Soc. Am.* **1991,** *8,* 2021–2025.

[9] Knoesen, A.; Moharam, M.G.; Gaylord, T.K. *Appl. Phys. B: Photophys. Laser Chem.* **1985,** *38,* 171–178.

[10] Stathopoulos, N.A.; Savaidis, S.P.; Rangoussi, M. *Opt. Quantum Electron.* **2006,** *38,* 683–699.

[11] Knoesen, A.; Gaylord, T.K.; Moharam, M.G. *J. Lightwave Technol*. **1988,** *6,* 1083–1104.

[12] Chou, C.; Sun, N. *J. Opt. Soc. Am.* **2008,** *25,* 545–554.

[13] Watkins, D.A. *Topics in Electromagnetic Theory*; John Wiley & Sons: New York, 1958.

[14] Pierce, J.R. *Travelling Wave Tubes*; Van Nostrand: New York, 1950.

[15] Sensiper, S. *Proc. IRE* **1955,** *43,* 149–161.

[16] Singh, U.N.; Singh, O.N.II; Khastgir, P.; Dey, K.K. *J. Opt. Soc. Am.* **1995,** *12,* 1273–1278.

[17] Siong, C.C.; Choudhury, P.K. *J. Electromagn. Waves Appl.* **2009,** *23,* 663–674.

[18] Kapoor, A.; Singh, G.S. *J. Lightwave Technol.* **2000,** *18,* 849–852.

[19] Safaai-Jazi, A.; Yip, G.L. *Radio Sci.* **1977,** *12,* 603–609.

[20] Snitzer, E. *J. Opt. Soc. Am.* **1961,** *51,* 491–498.

Downloaded by [Manish Kumar] at 02:04 05 October 2013